OSCILLATING SUPERLEAK TRANSDUCERS FOR QUENCH DETECTION IN SUPERCONDUCTING ILC CAVITIES COOLED WITH HE-II*

Z. A. Conway#, D. L. Hartill, H. S. Padamsee, and E. N. Smith
CLASSE, Cornell University, Ithaca, New York, USA

Abstract

Quench detection for 9-cell ILC cavities is presently a cumbersome procedure requiring two or more cold tests. One cold test identifies the cell-pair involved via quench field measurements in several pass-band modes. A second test follows with numerous fixed thermometers attached to the culprit cell-pair to identify the particular cell. A third measurement with many localized fixed thermometers is necessary to zoom in on the quench spot. We report here on a far more efficient alternative method which utilizes a few (e.g. 8) oscillating superleak transducers to detect the He-II second sound wave driven by the defect induced quench. Using a 9-cell reentrant cavity we identified the quench location in one cold test by powering several modes of the fundamental pass-band. Results characterizing the defect location with He-II second sound detection and corroborating measurements with carbon thermometers will be presented.

INTRODUCTION

14,560 superconducting niobium 9-cell cavities are required for the International Linear Collider (ILC) [1], each of which must have an accelerating gradient of 35 MV/m to pass the acceptance test. Due to major R&D efforts by many laboratories within the TESLA Technology Collaboration (TTC) DESY has now successfully tested more than 12 cavities over 35 MV/m [2]. Nevertheless the means for reliably producing cavities which achieve accelerating gradients >35 MV/m with a high yield remains to be demonstrated as one of the ILC highest priority R&D goals. Frequently, the cavity gradients are limited by defects on the RF surface which quench at field levels well below 35 MV/m. Such quench limited cavities may be repairable but the process of locating defects in 9-cell cavities remains a lengthy and cumbersome process.

Many laboratories are developing large scale thermometry systems to pin-point the quench locations. Here, we present a cost-effective and simple method to detect quench locations. By testing a superconducting cavity in a superfluid helium (He-II) bath it is possible to observe second-sound temperature waves driven by the conversion of stored RF energy to thermal energy at the defect [3, 4]. By experimentally measuring the time-of-arrival of the second sound wave at three or more detectors the location of the defect can be determined. Here, we use oscillating superleak transducers (OST), which measure the fluctuating counterflow velocity [5, 6, 7], to detect the time of arrival of second sound waves. Due to the ~20 m/s velocity of a He-II second sound wave over a wide temperature range the second sound wave time-of-flight over distances of a few millimeters is easily determined [7] The second sound signal is more easily visible at 1.8K than 2K because the superfluid density is nearly 50%. .

The remainder of this paper is split into four parts. First, we briefly discuss the RF performance history of the 9-cell reentrant cavity used in the experimental work. Next, we present the second-sound time-of-flight results used to locate the defect. Third, we show results of direct thermometric measurements of the cavity outer surface which corroborate the second sound defect location. Finally, we conclude with a few closing comments about our future plans.

RESONATOR TESTING

Resonator Processing and RF Performance

After fabrication at AES (Medford, NY) the initial chemical processing of the 9-cell reentrant cavity was performed in early 2007 [8]. This included final vertical EP 25 μm and a bake at 110^0C for 48 hours. After cooling the cavity to 2 K, the RF performance shown in figure 1 was measured (July 2007 curve). The cavity operated cw at accelerating gradients up to 14.6 MV/m where the cavity quenched. This accelerating gradient corresponds to a peak surface magnetic field of 549 Oe and a peak surface electric field of 35 MV/m [9].

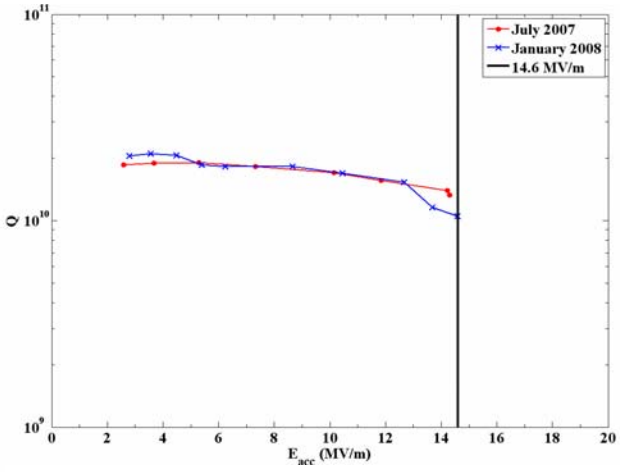

Figure 1: 9-cell reentrant cavity test results.

*Work supported by NSF and DOE
zac22@cornell.edu

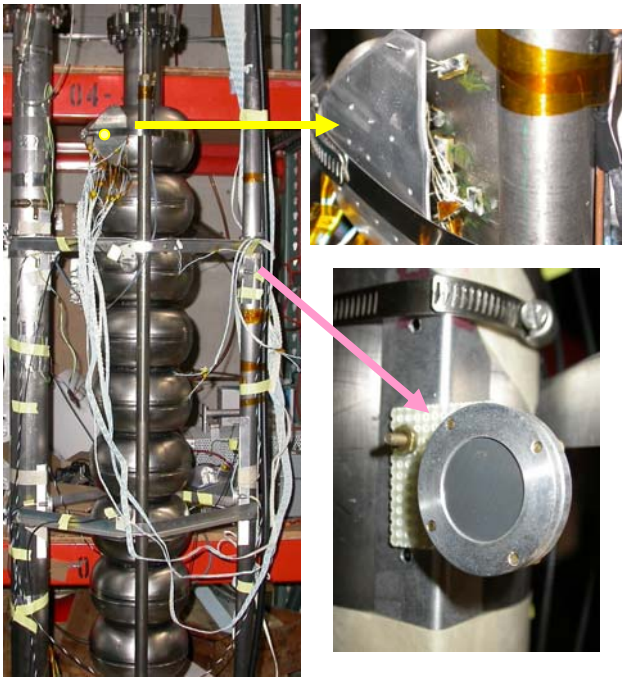

Figure 2: (Left) The 9-cell reentrant cavity ready for testing. 6 of the 8 OSTs and the fixed thermometer array are visible. The yellow circle corresponds to the defect location identified. (Top Right) A side view of the fixed thermometer array used to verify the accuracy of the second sound quench detection. (Lower Right) One of the 8 oscillating superleak transducers used to locate the defect.

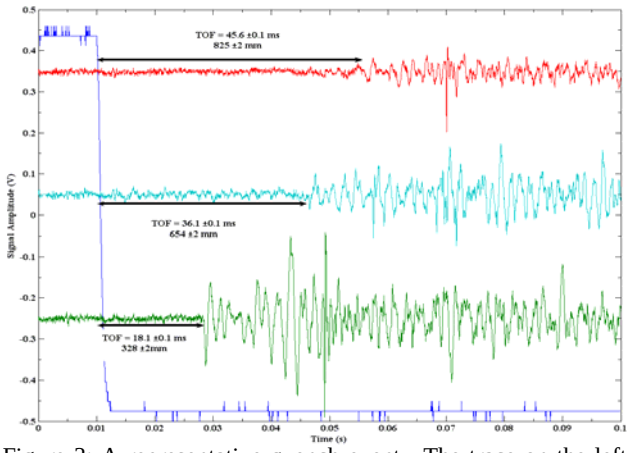

Figure 3: A representative quench event. The trace on the left (blue) shows the transmitted RF signal at quench. The upper three traces show the OST signals delayed by a time corresponding to their respective distances from the quench location.

Immediately following the initial test which found the cavity RF field amplitude to be quench limited, two programs were implemented: 1) perform a heavy EP, to remove enough material to repair the cavity and 2) locate the defect should the EP repair prove ineffective. Item 2 will be discussed in the next section.

First, the cavity received a series of heavy vertical electropolish procedures to remove 125 μm of material from the RF surface. The EP procedures were followed with a 48 hour 600^{0}C bake at FNAL. After another light EP etch (20 μm), HPR cleaning and 110^{0}C bake the cavity was again cooled to 2 K and tested. It was found that the cavity RF performance was unchanged, figure 1.

Second Sound Defect Location

The abrupt dissipation of the stored RF energy during quench is a symptom of a stubborn surface defect. To locate the defect an array of 8 OST were employed. The 8 OST were subdivided into two geometrically similar square arrays with one OST at each corner and ~17.2 cm from the cavity beam axis to each OST. One square array was located around the equator weld of the third cell and the OST of the second square array was ~11 cm above the equator weld of the sixth cell. Refer to figure 2 for details.

The measured time-of-arrival of the second sound wave at each OST is determined by the second sound wave time-of-flight from the defect heated region to the OST. By measuring the time-of-flight to three or more OSTs at different positions around the cavity, the location of the defect can be unambiguously determined [8]. It is important to note that this method requires only a single cavity test to locate, in three dimensions, surface defects which result in quench.

A single quench event at 1.94 K is shown in figure 2. The step-like trace on the left-hand side of the graph is the transmitted power signal output from an HP 423A crystal detector. The cavity π-mode was excited with an RF-pulse to a peak accelerating gradient of 14.6 MV/m, causing a cavity quench. The additional three traces display the second sound wave fluctuating counterflow velocity as measured by three of the OSTs. The location of the three OSTs and the defect location are highlighted in figure 3.

In addition, to the above event other modes of the cavity 1.3 GHz pass-band were excited at various He bath temperatures. In each case the cavity was found to quench at the same location.

Thermometric Defect Location

Once the defect was located with second sound, another 2 K RF test focused on confirming the defect location with traditional carbon thermometers. A special plate, which conformed to the reentrant cell shape, was fitted with an array of 15 Allen-Bradley 100 Ω, 1/10 W, carbon resistors. This thermometer assembly was pressed with spring loaded contacts (pogo sticks) onto the cavity outer surface to map the temperature of the defect region.

Due to a failure of the input coupler feedthrough from very high power application during the previous test we were only able to weakly couple to the cavity during the fixed thermometry test. The maximum achievable accelerating gradient was limited to 8 MV/m in the cell with the defect. However, this was still sufficient for the measurement of a temperature map of the cavity surface around the defect location with 15 fixed thermometers. Four out of the 15 thermometers showed defect heating.

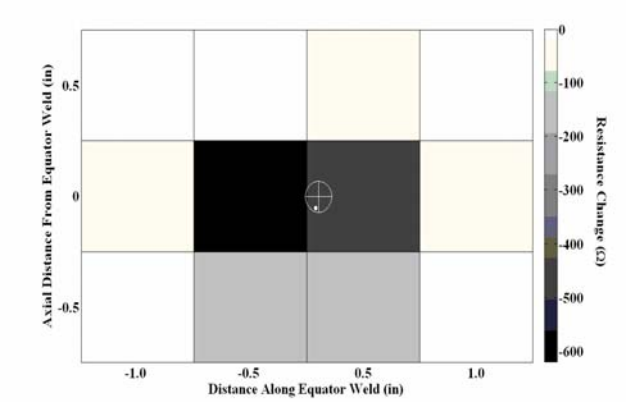

Figure 4: A thermal map of the cavity outer surface around the defect location. The horizontal axis corresponds to the distance along the weld and the vertical axis corresponds to the distance away from the weld. Each square represents one thermometer. The shading scale is shown on the right. The maximum resistance change of 600 Ω corresponds to a thermometer signal of about 50 mK during defect heating at 8 MV/m. The optically located defect is shown with a solid white circle. The center of the cross is where the second sound measurements located the defect; the circle around the cross has a radius of 3mm.

The other thermometers showed no temperature rise as expected below quench.

Figure 4 shows the thermometer array spacing and the measured heating. The horizontal axis is the distance along the equator weld and the vertical axis is the distance away from the equator weld. Each square represents the measurement of a single thermometer. The maximum resistance change of 600 Ω corresponds to a thermometer signal of about 50 mK during defect heating at 8 MV/m.

There are 3 distinct sets of data shown in figure 4: 1) the results of a direct thermometric measurement of the cavity temperature (described in this section), 2) the results of the second sound quench location (described in the previous section), and 3) the results of an optical inspection of the cavity RF surface (discussed in the next section). The second sound telemetry results for the quench location are highlighted with a cross and surrounded by a circle of 3 mm radius. The solid white circle in the lower left quadrant of the cross is centered over a pit located by optically inspecting the cavity RF surface, discussed in the next section. Note that the defect locations determined by the thermometric measurement, the second sound time-of-flight measurements, and the optically located defect were all in reasonably good agreement.

Figure 6: (Top)Questar long-distance microscope inspection equipment. (Top Left) Questar, (Top Middle) cylinder/mirror assembly (the mirror is not visible). (Bottom) Mirror and light used to view cavity interior.

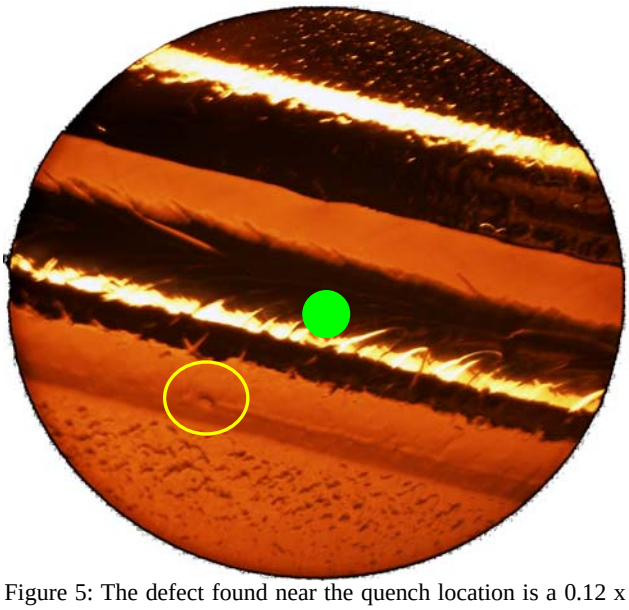

Figure 5: The defect found near the quench location is a 0.12 x 0.06 mm pit on the weld (highlighted with a yellow circle, about 0.6 mm diameter). The solid green circle corresponds to where the second sound measurement located the defect. The weld appears shiny in the middle and matt at the edge due to the lighting quality. The large grains of the heat affected zone are visible outside the weld.

INSPECTION

Optical inspection of the cavity RF surface using a Questar long-distance microscope found a small pit where the second sound telemetry located the defect, figure 5. The defect is elliptical in shape with a 0.12 mm major radius and a 0.06 mm minor radius. For reference, a large green circle was added to the figure where the second sound measurements located the defect.

Figure 6 shows the equipment used to optically inspect the cavity RF surface. The Questar long-distance microscope is on the left. Coaxial with the cavity is a white cylinder, which contains an integral mirror and light source for viewing the inner surface of the cavity.

SUMMARY

We presented a method which can locate a quench site on the RF surface of a superconducting niobium 9-cell cavity which requires a single cold test. This was achieved by measuring the time-of-flight of He-II second sound waves, which are driven by the conversion of

electrical to thermal energy at the defect. The quench location by second sound was confirmed by traditional thermometry and optical inspection to be less than 3mm away from the defect.

The He-II second sound telemetry technique was verified with a direct thermometric mapping of the cavity outer surface temperature. Subsequent optical inspections revealed a small pit on the equator weld. Future centrifugal barrel polishing will be employed to remove the defect and possibly others like it.

ACKNOWLEDGEMENTS

Many thanks to Nick Szabo for his help in preparing and tesing the 2nd sound transducers and electronics in the Physics 510 teaching laboratory. A special thanks to Mathias Liepe and Grigori Eremeev for their late night help in RF tests.

REFERENCES

[1] N. Phinney, N. Toge, and N. Walker, eds., "International Linear Collider Reference Design Report, Volume 3: Accelerator," Pg. 14, (2007).

[2] L. Lilje, "R&D In RF Superconductivity To Support The International Linear Collider," PAC 07, Albuquerque, NM, June 2007, THXKI01, Pg. 2559 (2007).

[3] K.W. Shepard, C.H. Scheibelhut, R. Benaroya, and L.M. Bollinger, "Split Ring Resonator For The Argonne Superconducting Heavy Ion Booster," IEEE Trans. Nuc. Sci., NS-24, Pg. 1147 June 1977.

[4] K.W. Shepard, C.H. Scheibelhut, P. Markovich, R. Benaroya, and L.M. Bollinger, "Development And Production Of Superconducting Resonators For The Argonne Heavy Ion Linac," IEEE Trans. Mag., MAG-15, Pg. 666, Jan. 1979.

[5] R.A. Sherlock and D.O. Edwards, "Oscillating Superleak Second Sound Transducers," Rev. Sci. Instrum. 41, Pg. 1603 (1970).

[6] R. Williams, S.E.A. Beaver, J.C. Fraser, R.S. Kagiwada, and I. Rudnick, "The Velocity Of Second Sound Near T_λ," Phys. Lett. 29A, Pg. 279 (1969).

[7] D. L. Hartill et al., To Be Published.

[8] H. Padamsee, et al., "Results On 9-Cell ILC and 9-Cell Re-Entrant Cavities," PAC 07, Albuquerque, NM, June 2007 ,WEPMS009, Pg. 2343 (2007).

[9] V. Shemelin and H. Padamsee, "Superconducting Multicell Cavity With Rentrant Cells," Cornell LEPP SRF Note SRF050808-06 (2005).